Available online at www.sciencedirect.com
SCIENCE DIRECT®
Journal of Power Sources 119–121 (2003) 581–584
JOURNAL OF POWER SOURCES
www.elsevier.com/locate/jpowsour

Structural and electronic modifications induced by lithium insertion in Sn-based oxide glasses

Florent Robert[a], Françoise Morato[a], Jérôme Chouvin[a], Laurent Aldon[a], Pierre Emmanuel Lippens[a], Josette Olivier Fourcade[a], Jean-Claude Jumas[a,*], Bernard Simon[b], Philippe Biensan[b]

[a]*Laboratoire des Agrégats Moléculaires et Matériaux Inorganiques (UMR 5072 CNRS), Université Montpellier II, CC15 Place Eugène Bataillon, Montpellier 34095 Cedex 5, France*
[b]*SAFT, Direction de la Recherche, 111 Boulevard Alfred Daney, Bordeaux 33074 Cedex, France*

Abstract

The irreversible mechanisms of lithium insertion in amorphous tin composite oxides $SnB_{0.6}P_{0.4}O_{2.9}$ have been studied by X-ray diffraction (XRD) and ^{119}Sn Mössbauer spectroscopy. The determination of the Lamb–Mössbauer factor has allowed us to evaluate the relative numbers of different tin atoms (Sn^{II}, Sn^{0}). We show that insertion of lithium reduces the Sn^{II} into Sn^{0} atoms, which form nanoparticles of active species. The lithium ions act as glass modifiers, breaking the bonds within M–O–M′ (M, M′ = B, P, Sn) bridges and forming non-bridging $M–O^{\delta-}$ bonds.

Keywords: Anode material; Lithium batteries; Tin composite oxide; ^{119}Sn Mössbauer spectroscopy

1. Introduction

The increasing demand of electric energy for many applications motivates an intensive research for batteries. Lithium ion batteries are very promising due to their performances at different levels: specific capacity, cyclability, large reversibility and good safety. The research of new materials for negative electrodes knows a new interest through tin-based composite oxide glasses (TCO) [1,2] which show high electrochemical performances as negative materials with significantly higher reversible capacity as compared to carbon-based materials. The TCO are expected to absorb volume variation [3] of the active species when they are homogenously dispersed ex situ into the matrix of inactive components at nanoscale. The main problem is the large irreversible capacity (plateau) for the first discharge (≅300 mAh/g).

In this paper, we propose a detailed analysis of the reduction mechanisms in $SnB_{0.6}P_{0.4}O_{2.9}$ for the insertion of less than 2 Li per formula during the first discharge. This study offers interesting possibilities for a better understanding of the redox insertion process in TCO.

2. Experimental

The tin oxide composite glass $SnB_{0.6}P_{0.4}O_{2.9}$ is prepared by solid-state reaction. Stoichiometric amounts of SnO (synthesized at laboratory [4]), $H_2PO_4NH_4$ (P_2O_5 precursor) and B_2O_3 (from Aldrich) were dry blended and heated in a vitreous carbon heating boat inside a horizontal tube furnace. The sample was first heated at 180 °C for 15 h so as to avoid the quick decomposition of $H_2PO_4NH_4$ into P_2O_5, NH_3 and H_2O, then heated at 800 °C for 15 h in a constant flow of argon and quenched to room temperature by removing the heating boat from the furnace. The glass formed was almost clear and gave off a white powder after grinding.

X-ray diffraction (XRD) powder patterns were recorded on a Philips instrument, using Cu Kα radiation (λ = 1.5418 Å). The samples were prepared inside a glove box, by carefully opening the cells and placing the products on a glass sample-holder. The recordings were carried out under dynamic vacuum in order to avoid undesirable reactions with air.

^{119}Sn Mössbauer spectra were recorded by transmission in the constant acceleration mode using an EG&G spectrometer, equipped with a cryostat to work at low temperatures (down to 4 K). The absorbers, containing 1–2 mg of ^{119}Sn per cm^2, were prepared by mixing powder samples and

* Corresponding author. Tel.: +33-4-67-14-33-46; fax: +33-4-67-14-33-4.
E-mail address: jumas@univ-montp2.fr (J.-C. Jumas).

0378-7753/03/$ – see front matter © 2003 Elsevier Science B.V. All rights reserved.
doi:10.1016/S0378-7753(03)00294-5

apiezon grease inside the glove box, and sealed with parafilm to avoid contact with air. The source was ^{119m}Sn in a $BaSnO_3$ matrix. The velocity scale was calibrated using the magnetic sextet of a high purity iron foil absorber as a standard, using ^{57}Co (Rh) as the source. The spectra were fitted to Lorentzien profiles by least-squares method using the G.M.5.S.I.T program [5,6], the fit was quality controlled by the classical χ^2-test. Isomer shift values are given relative to the centre of the $BaSnO_3$ spectrum recorded at room temperature.

The discharge/charge curves were measured by means of Mac Pile system operating in a galvanostatic mode at current density of 10 mA/g between 3 and 0.1 V versus lithium. The electrochemical cell consisted of lithium disk (anode) and the TCO (cathode). The electrolyte was $LiPF_6$ (1M) in PC/EC/3DMC.

3. Results and discussion

3.1. X-ray diffraction

Fig. 1 shows the first electrochemical discharge curve obtained by using $SnB_{0.6}P_{0.4}O_{2.9}$ as active electrode material. The points A and B correspond to the insertion of 1.38 and 2.06 lithium, respectively. These two points are in the irreversible part of the discharge curve, the reversible insertion mechanism is observed for more than about four lithium. Fig. 2 shows the X-ray diffraction patterns of the samples A and B. For $SnB_{0.6}P_{0.4}O_{2.9}$ the XRD data shows the absence of long-range order in the pristine glass sample that confirms its amorphous structure. The XRD data of the selected electrode samples prepared by interrupting the discharge experiments of Li/$LiPF_6$/TCO cells are also included.

As expected, at 2.06 Li/Sn (sample B) the pattern clearly shows an amorphous characteristic diagram with large diffusion regions whose positions may be assigned to

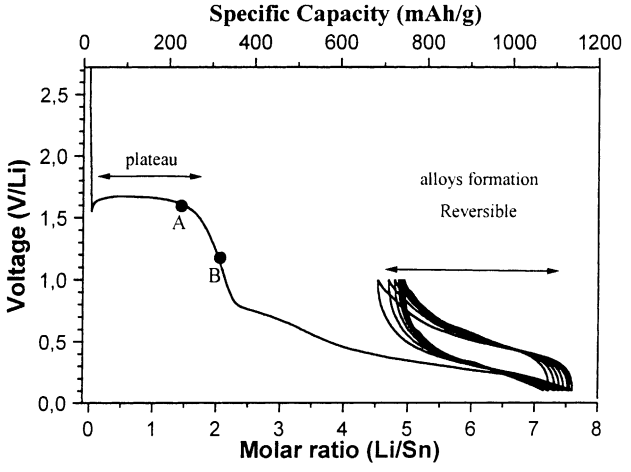

Fig. 1. First charge curve obtained with $SnB_{0.6}P_{0.4}O_{2.9}$ glass as active electrode material.

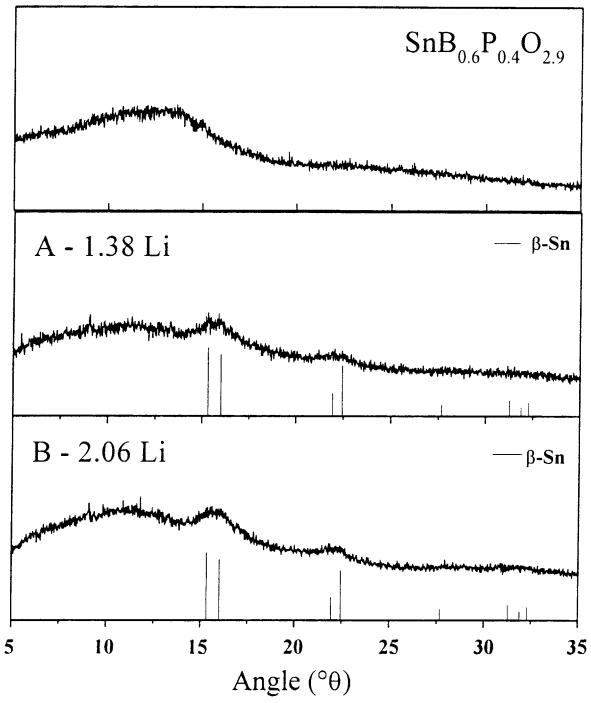

Fig. 2. X-ray diffraction patterns of the $SnB_{0.6}P_{0.4}O_{2.9}$ glass with different amounts of lithium for the first charge (Cu Kα, $\lambda = 1.5418$ Å).

β-Sn nanoparticles. The highly dispersed nature of the particles is clearly evidenced by the low signal/noise ratio and the broadened profiles.

3.2. ^{119}Sn Mössbauer spectroscopy

3.2.1. Pristine tin-based glass material

A deeper insight on the local environment of tin atoms in the non-crystalline solids is obtained by ^{119}Sn Mössbauer spectroscopy. Fig. 3 shows both the experimental data and the fitted curves (with two different tin sites) of the Mössbauer spectra for $SnB_{0.6}P_{0.4}O_{2.9}$ at room temperature and liquid nitrogen. The hyperfine parameters are given in Table 1. The averaged values of the isomer shift δ and quadrupole splitting Δ obtained for the two tin sites are close to those reported in the literature for Sn^{II} non-crystalline materials [7–9]. The contributions C_i of these two tin sites to the Mössbauer spectra which correspond to the relative area of the sub-spectra are also given. The relative numbers of tin sites n_i within the glasses are obtained by considering the Lamb–Mössbauer factor f_i by the relation:

$$n_i = \frac{C_i/f_i}{\sum C_j/f_j} \quad (1)$$

where the summation is on all the tin sites. As expected, the value of δ is found to increase with the decreasing temperature. The evaluation of f_i within the thin absorber approximation [10] from the variations of the sub-spectra area as a function of the temperature has been carried out. The values of f_i and n_i are given in Table 1. The two values of n_1 (and n_2) at

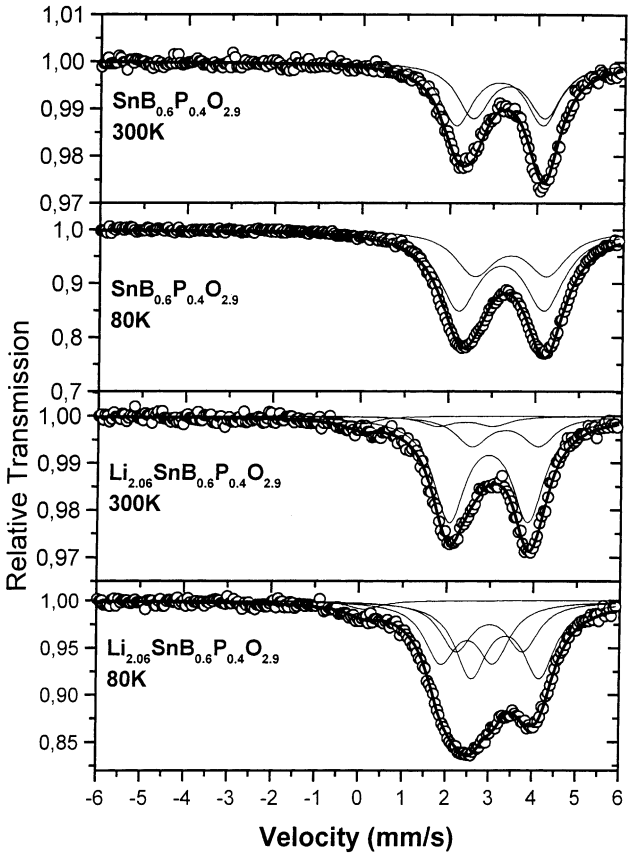

Fig. 3. ^{119}Sn Mössbauer spectra for: (a) $SnB_{0.6}P_{0.4}O_{2.9}$ at 300 K; (b) $SnB_{0.6}P_{0.4}O_{2.9}$ at 80 K; (c) $Li_{2.06}SnB_{0.6}P_{0.4}O_{2.9}$ at 300 K and (d) $Li_{2.06}SnB_{0.6}P_{0.4}O_{2.9}$ at 80 K.

80 and 300 K are equal within the experimental errors, which validates our approach. The number n_1 of Sn^{II} sites of type 1 is found to be about twice that of Sn^{II} sites of type 2. Based on the values of the hyperfine parameters we can tentatively ascribe two different local environments to the two types of tin atoms. The tin atoms of type 1, with large quadrupole splitting: $\Delta = 2.01$ mm/s (300 K) or $\Delta = 1.97$ mm/s (80 K) and the lower isomer shift $\delta = 3.12$ mm/s (300 K) or $\delta = 3.20$ mm/s (80 K), are expected to be bonded to bridging oxygen atoms (Sn–O–M with M = Sn, B, P) and can be considered as a network former. The tin atoms of type 2, with a lower quadrupole splitting: $\Delta = 1.66$ (300 K) or $\Delta = 1.67$ mm/s (80 K) and a higher isomer shift $\delta = 3.33$ (300 K) or $\delta = 3.41$ mm/s (80 K), are expected to be bonded to non-bridging oxygen ($Sn^{2+}\cdots O$) and can be considered as a network modifier.

3.2.2. Tin-based glass material electrodes after cell discharge

The same experimental procedure as described in Section 3.2.1 has been applied to the Li inserted sample B ($Li_{2.06}SnB_{0.6}P_{0.4}O_{2.9}$) which is considered only in this paper. The ^{119}Sn Mössbauer spectra at room temperature and liquid nitrogen are shown in Fig. 3 and the values of the hyperfine parameters are given in Table 1. The spectra can be interpreted by considering three main components: Sn^{II} site 1, Sn^{II} site 2 and Sn^0 and a very small amount (less than 3%) of Sn^{IV} which should be due to an accidental reoxidation. The contribution of the later component is not included in Table 1 for clarity. The relative numbers of tin sites n_i are reported in Table 1 and are found to be strongly different from the relative contributions to the Mössbauer spectra. This is mainly due to the differences in the f factors for the different tin sites especially at 300 K. It is worth noticing that the contribution of Sn^0 to the Mössbauer spectrum at 300 K is very small (<7%) compared to the relative number of sites (43%) because of the small value of the f factor (0.01). The values of n_i obtained at 80 and 300 K are consistent. There are 44% of Sn^0 in the lithiated compound resulting from the reduction of the Sn^{II} atoms.

Table 1
Hyperfine parameters obtained from the ^{119}Sn Mössbauer spectra shown in Fig. 3: the different types of tin used in the Mössbauer fitting procedure and their relative contributions in the Mössbauer spectra, the values of the isomer shift δ, the quadrupole splitting Δ and the Lamb–Mössbauer factor f, and the relative numbers of tin sites

Temperature (K)	Tin sites	Contribution (%)	δ (mm/s)	Δ (mm/s)	f	n_i
$SnB_{0.6}P_{0.4}O_{2.9}$						
300	Sn^{II} site 1	53.5	3.12	2.01	0.039	0.67
	Sn^{II} site 2	46.5	3.33	1.66	0.069	0.33
80	Sn^{II} site 1	63.4	3.20	1.97	0.420	0.67
	Sn^{II} site 2	36.6	3.41	1.67	0.490	0.33
$Li_{2.06}SnB_{0.6}P_{0.4}O_{2.9}$						
300	Sn^{II} site 1	70.6	2.95	1.81	0.313	0.15
	Sn^{II} site 2	20.6	3.32	1.54	0.031	0.42
	Sn^0	6.8	2.48	1.22	0.010	0.43
80	Sn^{II} site 1	26.8	2.99	1.53	0.734	0.15
	Sn^{II} site 2	41.1	3.37	1.57	0.398	0.41
	Sn^0	32.1	2.48	1.22	0.290	0.44

The Sn(IV) contribution for the lithiated compound is not included for clarity.

The Sn^0 are expected to be nearby β-Sn nanoparticles in agreement with the X-ray diffraction pattern (Fig. 1). However, the values of the hyperfine parameters ($\delta = 2.48$ and $\Delta = 1.22$ mm/s) show that the formed active species Sn^0 are in interaction with approximately 0.4 Li. This value corresponds to an average value estimated from the curve $\delta = f(x\mathrm{Li})$ and is found to be close to those usually observed in $Li_{0.5}$–Sn alloy: 2.49 mm/s < δ <2.54 mm/s (Table 1 in [11]). The rather high value of ($\Delta > 1$ mm/s) suggests interactions between the active species and oxygen of the glass matrix. Like this, over the 2.06 Li atoms, the reaction of $SnB_{0.6}P_{0.4}O_{2.9}$ with 1.06 Li induces the extraction with reduction of 0.44 Sn^{II} (site 1) into Sn^0. The Sn^0 atoms should be bonded to both Li and Sn atoms. The 0.88 Li^+ combine with terminal oxygen atoms of the modified network appropriate to the stoechiometry of the Li_2O formation in interaction with the glass network. This restructuring induces the formation of a zone rich in Sn^0 separated by a zone rich in ''Li_2O''. The remaining lithium (one Li atom) modifies the glass network and probably contributes to the formation of the solid electrolyte interface at the anode.

4. Conclusion

Insertion of lithium in $SnB_{0.6}P_{0.4}O_{2.9}$ can be described by two main mechanisms which are irreversible for less than about four Li and reversible for a larger amount. In this paper, we have only studied the first irreversible mechanism which strongly reduced the electrochemical performances of the anode material. We have shown from X-ray diffraction and Mössbauer experiments that insertion of lithium reduces 44% of the Sn^{II} atoms into Sn^0 which form nanoparticles of active species for the reversible mechanisms. The lithium ions act as glass modifiers breaking the bonds within the M–O–M′ (M, M′ = B, P, Sn) bridges and forming non-bridging $M–O^{\delta-}$ bonds.

Acknowledgements

The authors would like to thank the CNRS, France (PICS 505) and SAFT (Bordeaux, France) for financial support.

References

[1] Fuji Photo Film Co. Ltd., European Patent, EP 0 704 921 A1, 1995.
[2] Y. Idota, T. Kubota, A. Matsufuji, Y. Maekawa, T. Miyasaka, Science 276 (1997) 1395.
[3] H. Li, L. Shi, Q. Wang, L. Chen, X. Huang, Solid State Ionic 8263 (2002).
[4] J. Chouvin, C. Branci, J. Sarradin, J. Olivier-Fourcade, J.C. Jumas, B. Simon, Ph. Biensan, J. Power Sources 81–82 (1999) 277.
[5] K. Ruebenbauer, T. Birschall, Hyperfine Interact. 7 (1979) 175.
[6] S.L. Ruby, Mössbauer Effect Methodology 1973, 263.
[7] P.G. Appleyard, J.A. Johnson, C.E. Johson, M.F. Thomas, D. Holland, A. Sears, J. Phys. Condens. Matter 9 (1977) 7477.
[8] A. Paul, J.D. Donaldson, M.T. Donoghue, M.J.K. Thomas, Phys. Chem. Glasses 18 (1977) 125.
[9] J. Isidorson, C.G. Granqvist, L. Häggström, E. Nordström, J. Appl. Phys. 80 (1996) 2367.
[10] R.H. Herber, Phys. Rev. B 27 (7) (1983) 4013.
[11] J. Chouvin, J. Olivier-Fourcade, J.C. Jumas, B. Simon, O. Godiveau, Chem. Phys. Lett. 308 (1999) 413.